FATIGUE AND FRACTURE RESEARCH IN COMPOSITE MATERIALS

T. Kevin O'Brien
NASA Langley Research Center
Hampton, Virginia

INTRODUCTION

NASA Langley has a major research program to understand and characterize the fatigue, fracture, and impact behavior of composite materials (fig. 1). Bolted and bonded joints are included. The scope of this work is generic so that the solutions developed will be useful for a wide variety of structural applications. The analytical tools developed are used to demonstrate the damage tolerance, impact resistance, and useful fatigue life of structural composite components. Furthermore, much recent emphasis is on developing and analyzing standard tests for screening improvements in materials and constituents.

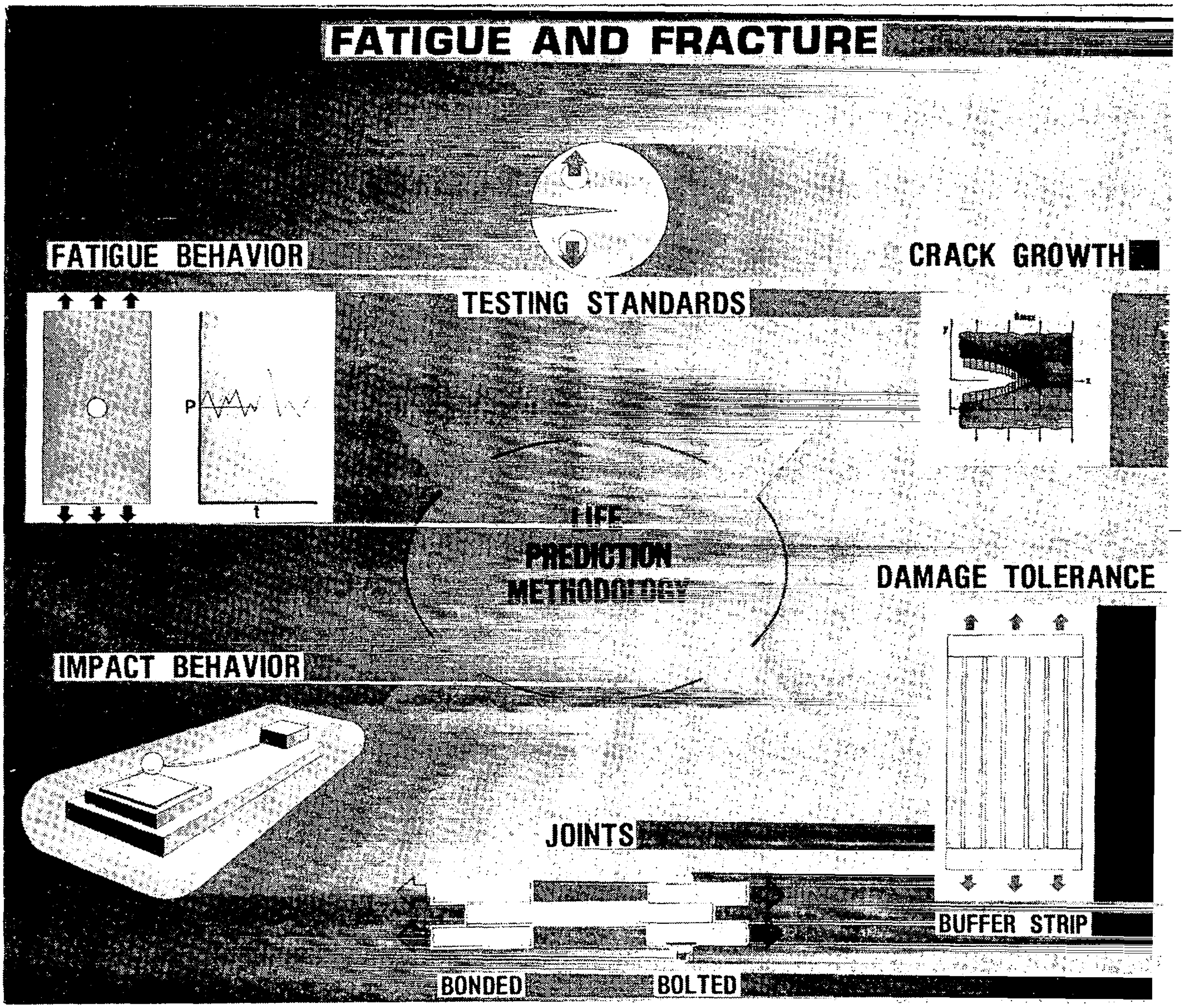

Figure 1

A UNIFYING STRAIN CRITERION TO PREDICT FRACTURE TOUGHNESS OF COMPOSITE LAMINATES

In references 1 and 2 a method was developed to predict composite fracture toughness from fiber and matrix properties. A laminate was assumed to fail when the strains at the crack tips in the principal load-carrying plies reach a critical level, regardless of layup. (See fig. 2.) The singular term in a series representation of the orthotropic strain field was chosen to represent the fiber strains. The fibers in the principal load-carrying plies were oriented at an angle θ to the applied load. The singular coefficient Q_c is given by $Q_c = K_Q\xi/E_y$, where K_Q is the usual stress intensity factor, E_y is the laminate modulus in the loading direction, and ξ is a function that depends only on the laminate elastic constants and the angle of the principal load-carrying plies. A critical level of strains at failure implies a constant value of Q_c, independent of ply orientations. Furthermore, Q_c is proportional to the ultimate tensile failing strain of the fibers, independent of the matrix material. (See fig. 2.) Therefore, the fracture toughness of all fibrous composite laminates can be computed from the ultimate tensile failing strain of the fibers and the elastic constants.

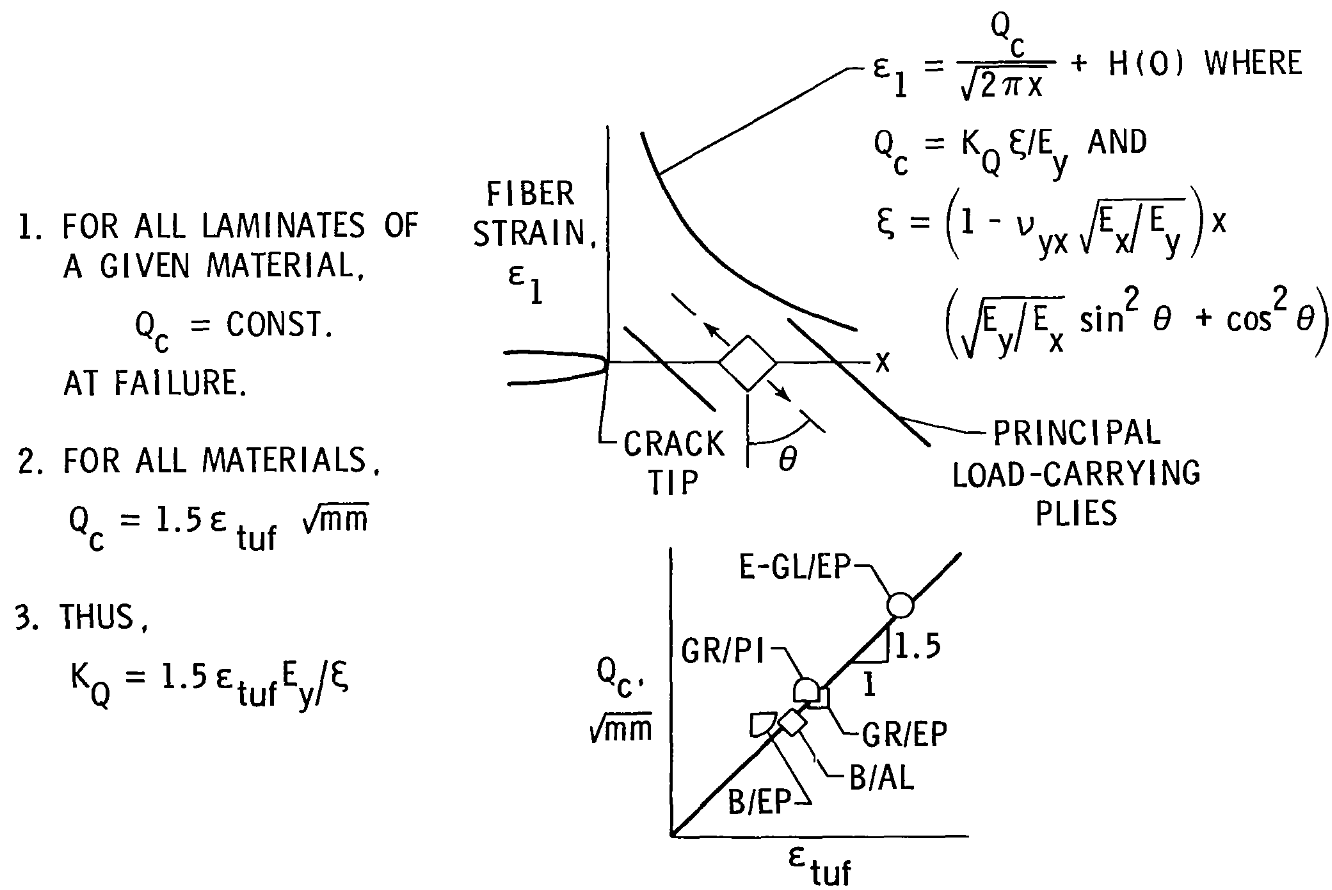

Figure 2

MEASURED AND PREDICTED VALUES OF FRACTURE TOUGHNESS

Figure 3 shows predicted and measured values of composite fracture toughness for a number of different layups and materials. The value of K_Q increases in proportion to fiber strength. Hence, the laminates with boron fibers have the highest K_Q and those with E-glass the lowest. The predictions, which are usually within 10 percent of the measurements, are quite good. The discrepancies between predicted and measured values of K_Q may be due largely to matrix and fiber failures at the crack tips that occur before overall failure. These crack tip failures, which alter the local fiber stresses, are not presently accounted for in the analysis. Micromechanical analyses are being developed that do account for these failures. In addition, experiments are being conducted to measure the type and extent of crack tip failures for various layups.

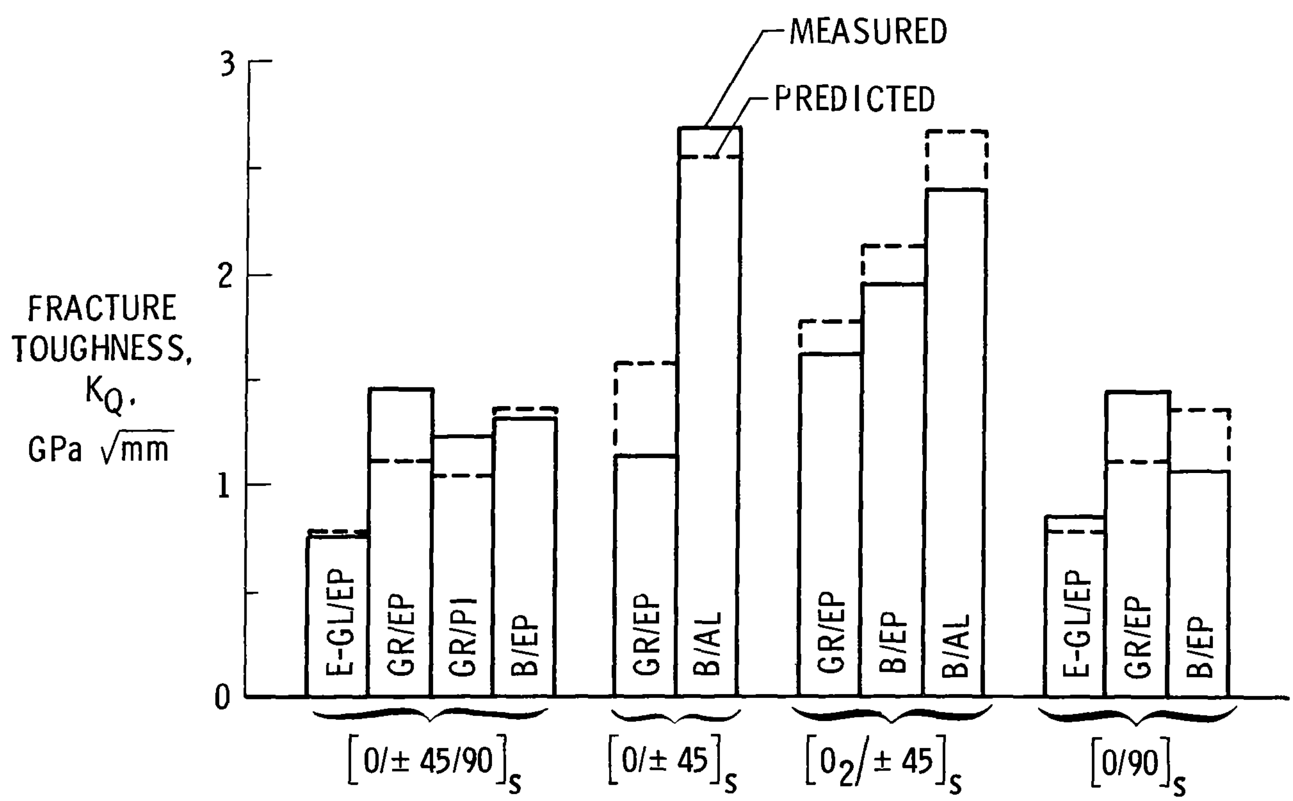

Figure 3

IMPROVING DAMAGE TOLERANCE OF COMPOSITE LAMINATES

WITH BUFFER STRIPS - TEST RESULTS

Buffer strips can greatly increase the tensile strength of damaged graphite/epoxy laminates while increasing weight only a little. In addition, recent work has shown that S-glass buffer strips can be woven into the 0° graphite plies with little additional expense (ref. 3). Figure 4 shows the remote strain for three quasi-isotropic panels containing center slits and S-glass buffer strips. Fracture initiates in panels with (filled symbols) and without (dashed curve) buffer strips at the same remote strain. However, the buffer strips arrest the fractures because they have a higher modulus of resilience than the graphite. The eventual failing strains of the panels are more than two times the strain at which the fracture initiated from the longest slit. Thus, in a damage tolerance situation, the strengths of these panels can be twice that of plain laminates.

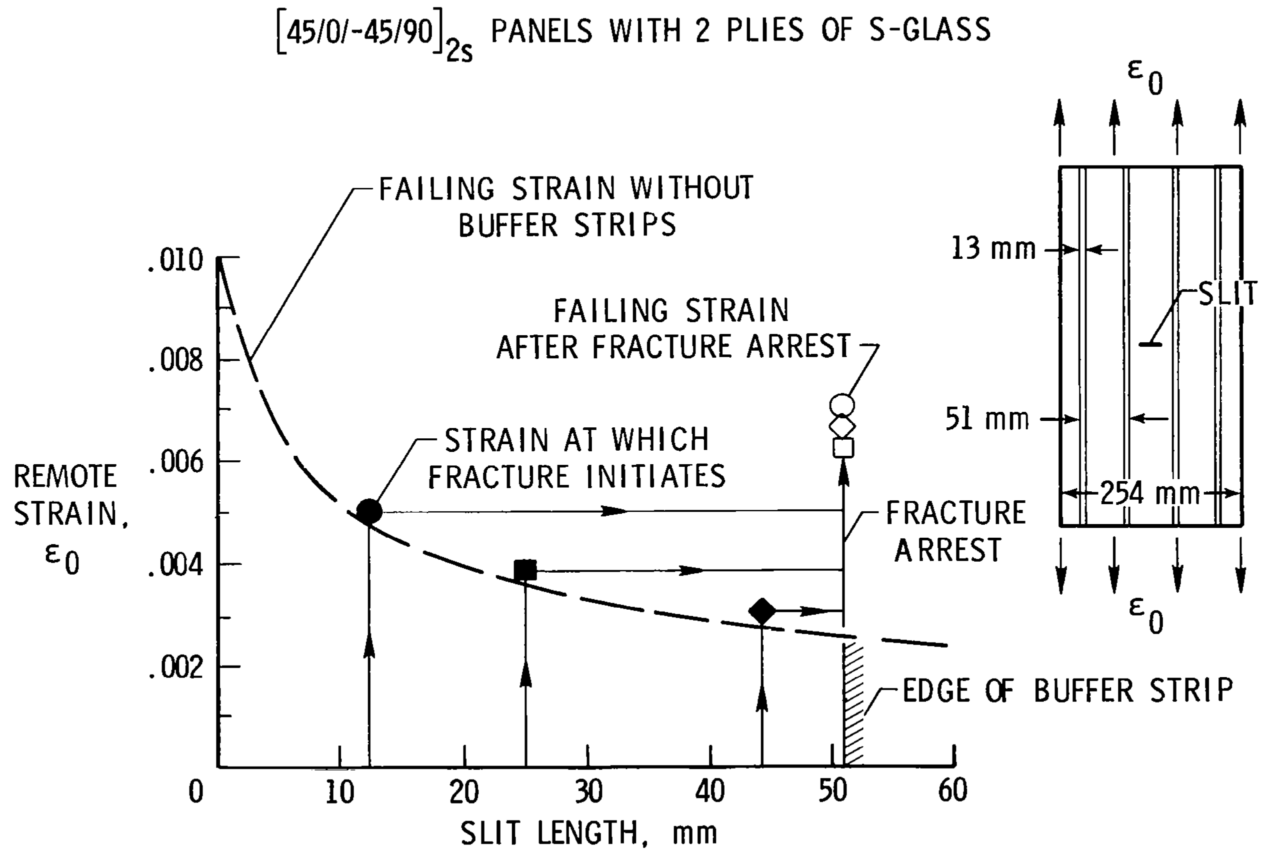

Figure 4

IMPROVING DAMAGE TOLERANCE OF COMPOSITE LAMINATES

WITH BUFFER STRIPS - ANALYSIS

In addition to the buffer strip panels in figure 4, panels were also made with other buffer materials, various numbers of buffer plies and spacings, and various layups (ref. 3). Figure 5 shows the ratios of cracked to uncracked strength for these tests plotted against the buffer strip spacing (which is the arrested crack length) multiplied by the ratios of number of 0° plies and modulus of resilience for graphite to buffer material. Each symbol represents an average of three tests. Round symbols represent S-glass buffer strips; square symbols represent Kevlar buffer strips. Filled and open symbols differentiate between the two layups (shown in the key) used for the main panel material. A shear-lag analysis indicates that for large values of the abscissa, the strength ratio should vary inversely with the square root of the abscissa. S-glass has the highest modulus of resilience, and hence gives the highest strengths. For small values of the abscissa, the strengths are limited to the ultimate net section strength, which is 75 percent of the uncracked strength. (The buffer strip spacing, W_a, is 25 percent of the panel width.) The test data agree very well with this relationship. Additional tests are currently being conducted for a wider range of buffer strip parameters and for woven buffer material. Tests are also being conducted to determine the influence of environment and fatigue loading on strengths. Furthermore, analyses are being developed to better predict the strengths in terms of the buffer strip parameters.

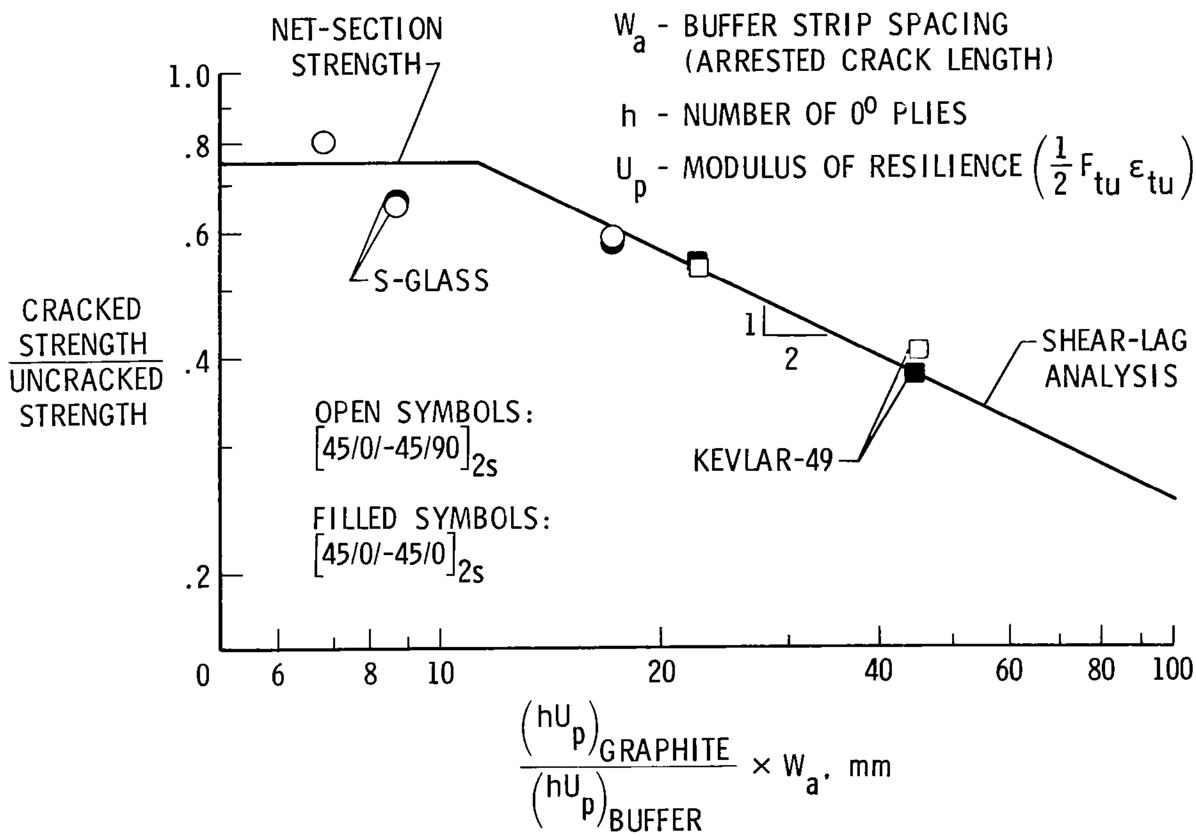

Figure 5

HOLE ELONGATION UNDER CYCLIC LOADING

IN BOLTED COMPOSITE JOINTS

Bolt holes in composite joints can elongate under cyclic loading and thereby reduce joint stiffness. Single-fastener joints were tested in reference 4 using different combinations of tension-tension fatigue loading and bolt clampup torques. Figure 6 shows measured hole elongations from three tests that produced about the same fatigue life. This figure shows the influence of clampup on hole elongation. For the case of pin bearing with no clampup constraint, the figure shows that the bolt hole did not elongate before it failed in fatigue. But with "finger-tight" clampup and a higher cyclic stress, the hole elongated extensively before it failed. Much less elongation is shown for the third case, which has a typical 2.82 N·m clampup for the 6.35-mm-diameter bolt. Other tests were conducted to measure hole elongation and strength under static loading. Future research will focus on analyzing damage mechanisms for bearing-loaded holes.

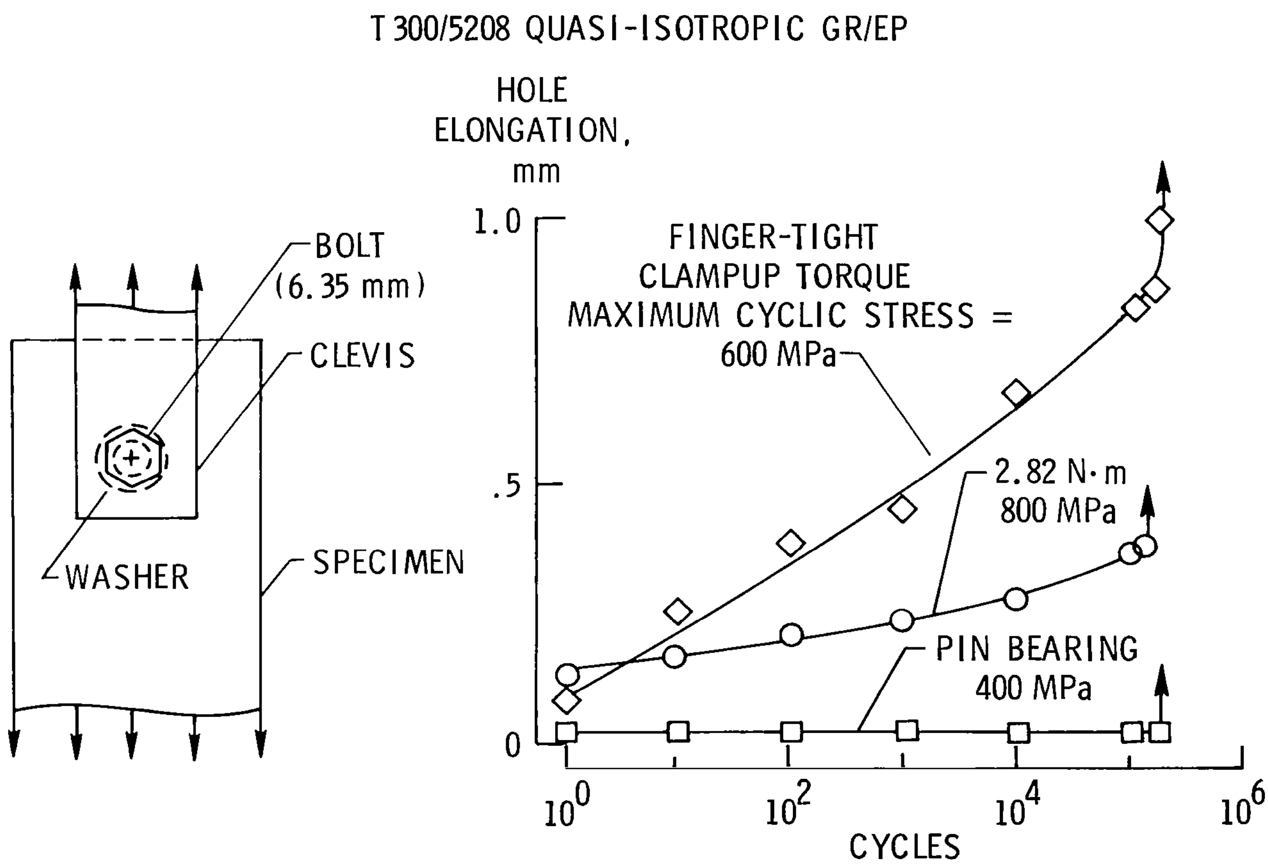

Figure 6

BOLT CLAMPUP RELAXATION

Recent studies have shown that bolt clampup improves the strength of composite joints. This improvement, however, may decrease somewhat if the bolt clampup force relaxes during long-term exposure. A viscoelastic relaxation analysis has been developed (ref. 5) for steady-state exposure conditions. A simple double-lap bolted joint was analyzed using a finite-element procedure. Typical results are shown as symbols in the accompanying figure 7. For the room-temperature-dry (RTD) reference case, relaxations of 8, 13, 20, and 30 percent were calculated for 1 day, 1 week, 1 year, and 20 years, respectively. As expected, moisture increased the clampup relaxation compared to the RTD case. Reference 5 also includes results for elevated-temperature exposures. In addition to the finite-element analyses, a simple empirical equation was developed to calculate clampup relaxation. First, this equation was fitted (dashed curve) to the RTD finite-element results to establish two constants (F_1 and n). Then the equation was generalized to account for moisture by substituting viscoelastic shift factors a_{TH} from the literature. The solid curves show that this equation agrees quite closely with the finite-element results. Recently, this equation was extended to account for transient environments (ref. 6).

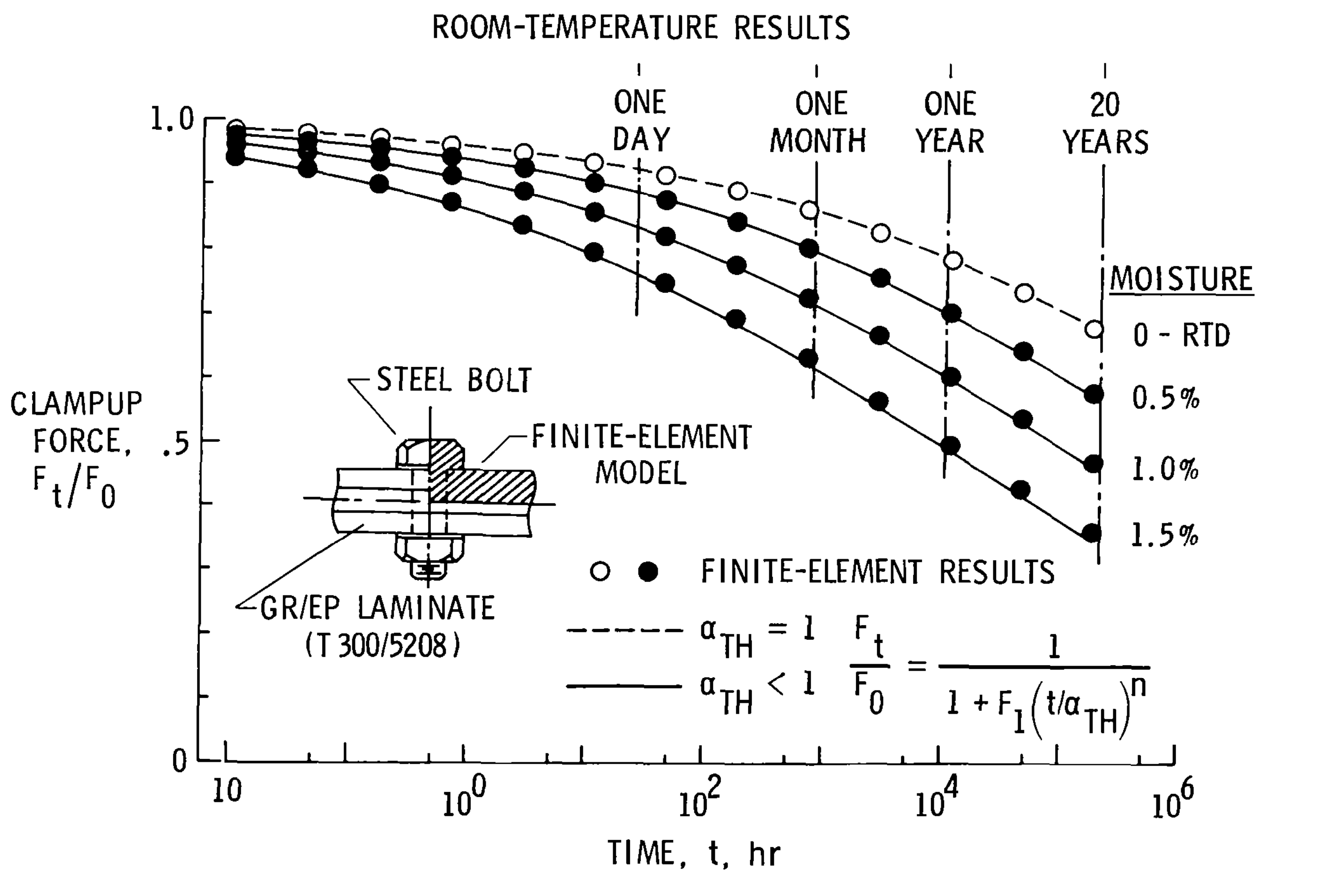

Figure 7

3-D STRESSES AT LAMINATE BOLT HOLES

High interlaminar stresses develop near holes in composite laminates. These interlaminar stresses were analyzed in reference 7 for a $[0/90]_s$ graphite/epoxy laminate with a circular hole and remote uniaxial loading. These stresses were calculated using a 3-D finite-element model with a very high mesh refinement near the ply interface. Typical stress results are presented in figure 8, and for convenience they are normalized by the remote stress S_g. The two curves in this figure represent the interlaminar normal and shear stresses, σ_z and $\sigma_{z\theta}$, respectively, along the hole boundary. These stresses provide a basis for locating delaminations at laminate holes. The 3-D finite-element procedures are currently being extended to calculate interlaminar stresses due to thermal and hygroscopic effects.

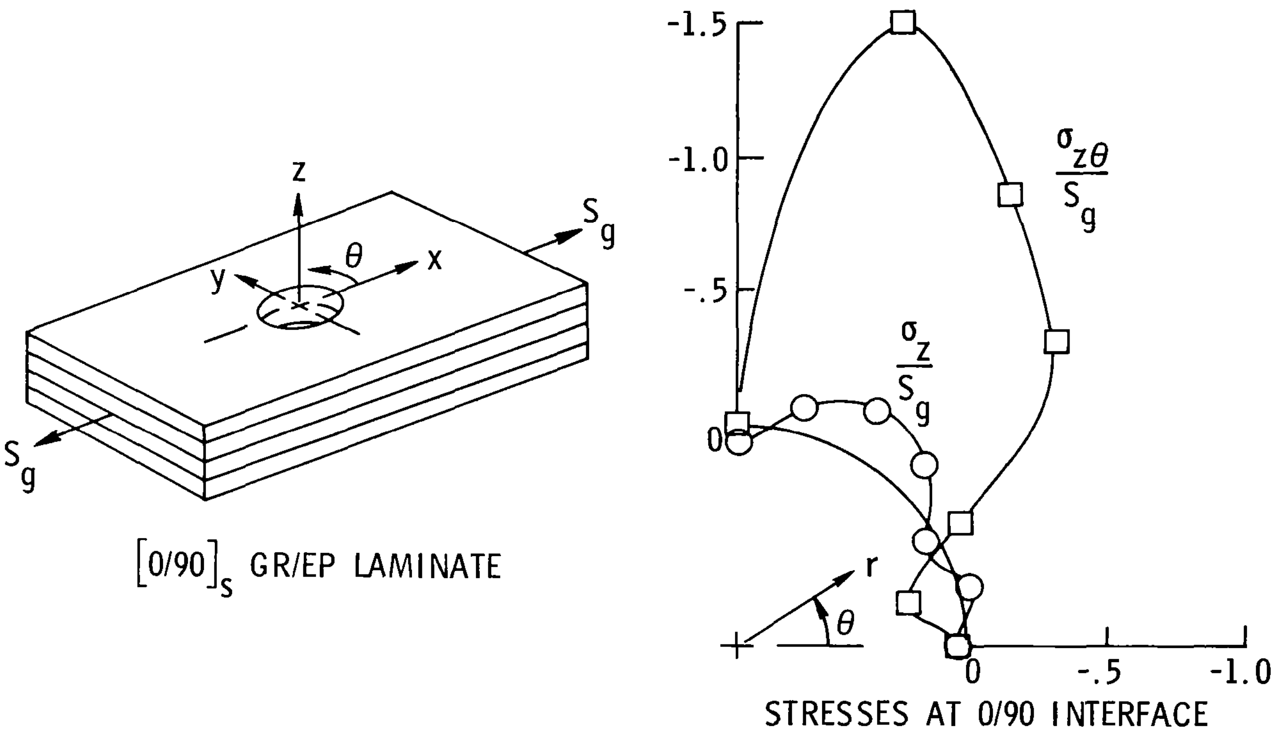

Figure 8

DAMAGE THRESHOLD UNDER LOW-VELOCITY

IMPACT OF COMPOSITES

Low-velocity impact can easily damage composite laminates by delaminating bonded layers or breaking fibers. Impact damage was studied to analyze the impact mechanics, determine failure criteria, and develop a simple impact test method. The test device consists of a hardened 1-inch-diameter steel ball at the end of a cantilevered rod (fig. 9). The ball strikes a 4-inch-square composite plate that is bonded to an aluminum support plate. The support plate has a circular aperture ranging in diameter from 1/2 to 3-1/2 inches. The ball and laminate are wired so that while they are in contact a circuit is completed and contact time is recorded on an oscilloscope. The expected impact duration, maximum impact force, and maximum shear and flexural stresses are calculated from an analysis based on the static first-mode deformations. The predicted durations and the test results agree within ±3 percent. The criteria for failure were found to be matrix ultimate shear stress and fiber ultimate stress. The right-hand figure shows that the analysis correctly predicts the damage threshold within about ±10 percent.

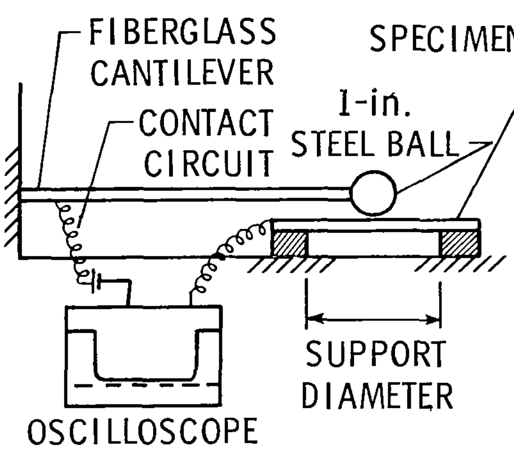

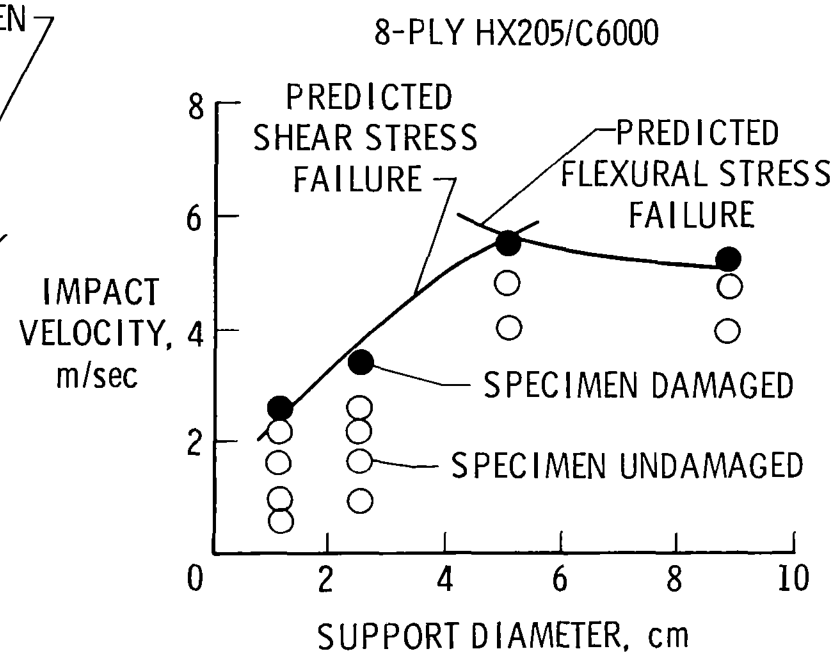

- MEASUREMENTS
  - VELOCITY OF IMPACT
  - DURATION OF IMPACT
- MODEL
  - DYNAMIC ANALYSIS OF DURATION, FORCE, ETC.
  - ONLY FIRST-MODE DEFORMATIONS CONSIDERED

- MODEL FAILURE PREDICTION AGREES WITH EXPERIMENT TO WITHIN ±10%

Figure 9

COMPOSITE IMPACT SCREENING BY STATIC INDENTATION TESTS

Graphite/epoxy laminates can lose up to 50 percent of their original strength from low-velocity impact damage. For laminates up to at least 16 plies, a static indentation test on a specimen bonded between two aperture plates yields failures almost identical to the failures from an impact (ref. 8). A static test, however, allows sufficient time for analysis of the failure sequence (fig. 10). The load deflection curve for an undamaged plate with a small span is shown in the left figure; the flexural stiffness from the shear strength of the matrix transfers most of the load to the supports. Damage progression occurs as matrix shear failure causes delaminations to grow, until only a membrane of delaminated fibers supports the load. Then membrane failure controls penetration load. For this configuration, matrix shear strength dominates the low-level impact damage, and the extent of delamination is limited by the fiber toughness. The figure on the right indicates that for larger aperture plates, failure is dominated by the failure energy of the overall membrane. Matrix failure, in this case, releases little energy; failure here is governed predominantly by fiber strength.

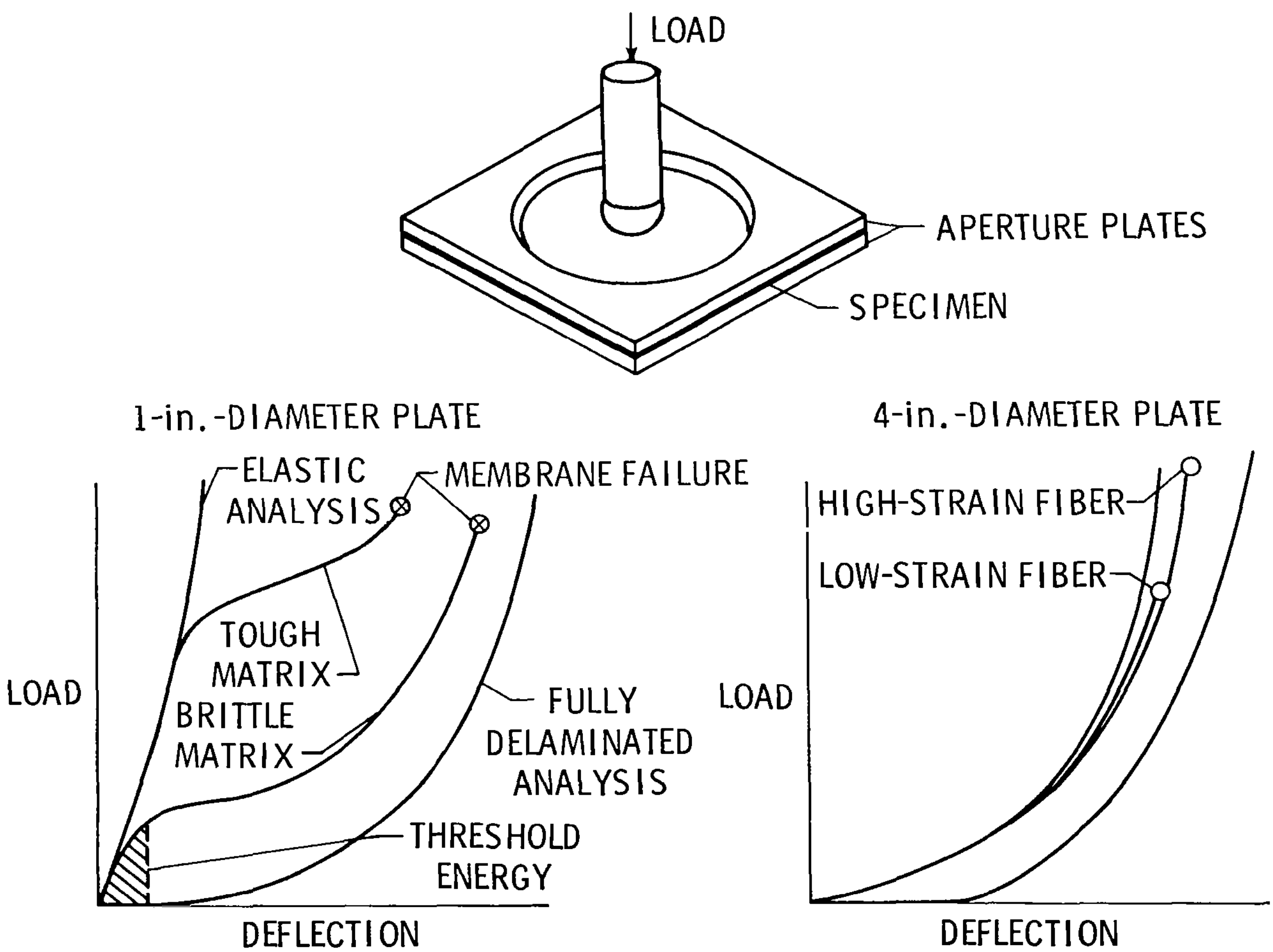

Figure 10

STRAIN ENERGY RELEASE RATE FOR DELAMINATION GROWTH DETERMINED

A simple expression was derived for the strain energy release rate, G, for edge delamination growth in an unnotched laminate (ref. 9). This simple expression shown in figure 11 has several advantages. First, G is independent of delamination size. It depends only on the applied strain, ε, the specimen thickness, t, the stiffness of the undamaged laminate, E_{LAM}, and the stiffness of the laminate when it was completely delaminated, E^*. Second, E_{LAM} and E^* can be calculated from simple laminated-plate theory. Third, because E^* depends on the location of the delaminated interface(s), E^*, and hence G, are sensitive to the location of damage in the laminate thickness. The simple equation was used to develop criteria to predict the onset and growth of delaminations in realistic, unnotched laminates.

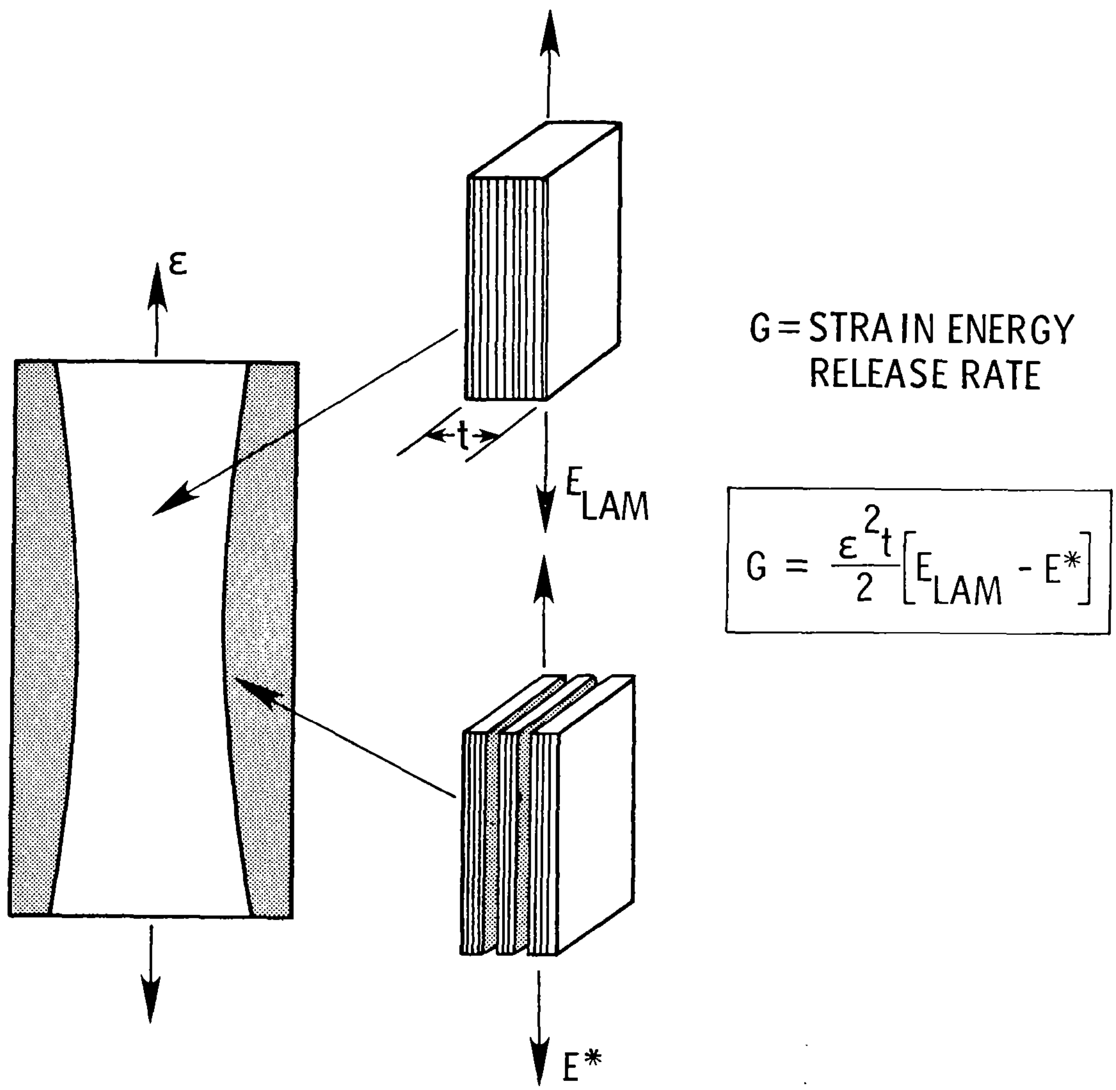

Figure 11

DELAMINATION ONSET PREDICTED

To predict the onset of delaminations in realistic unnotched laminates (ref. 9), quasi-static tension tests were conducted on the $[\pm 30/\pm 30/90/\overline{90}]_s$ laminates. The applied strain recorded at the onset of delamination, ε_c, was used to calculate a critical strain energy release rate, G_c. Then, G_c was used to predict the onset of delamination in more complex laminates. Figure 12 shows data and predictions for three $[+45_n/-45_n/0_n/90_n]_s$ laminates all having the same layup but with different ply thicknesses. For example, n = 1 is an 8-ply laminate, n = 2 is a 16-ply laminate, and n = 3 is a 24-ply laminate. The predictions agreed well with experimental data, indicating that G_c was a material property. Furthermore, the trend of lower ε_c for thicker laminates was correctly predicted. This trend could not be predicted by a critical interlaminar stress criterion.

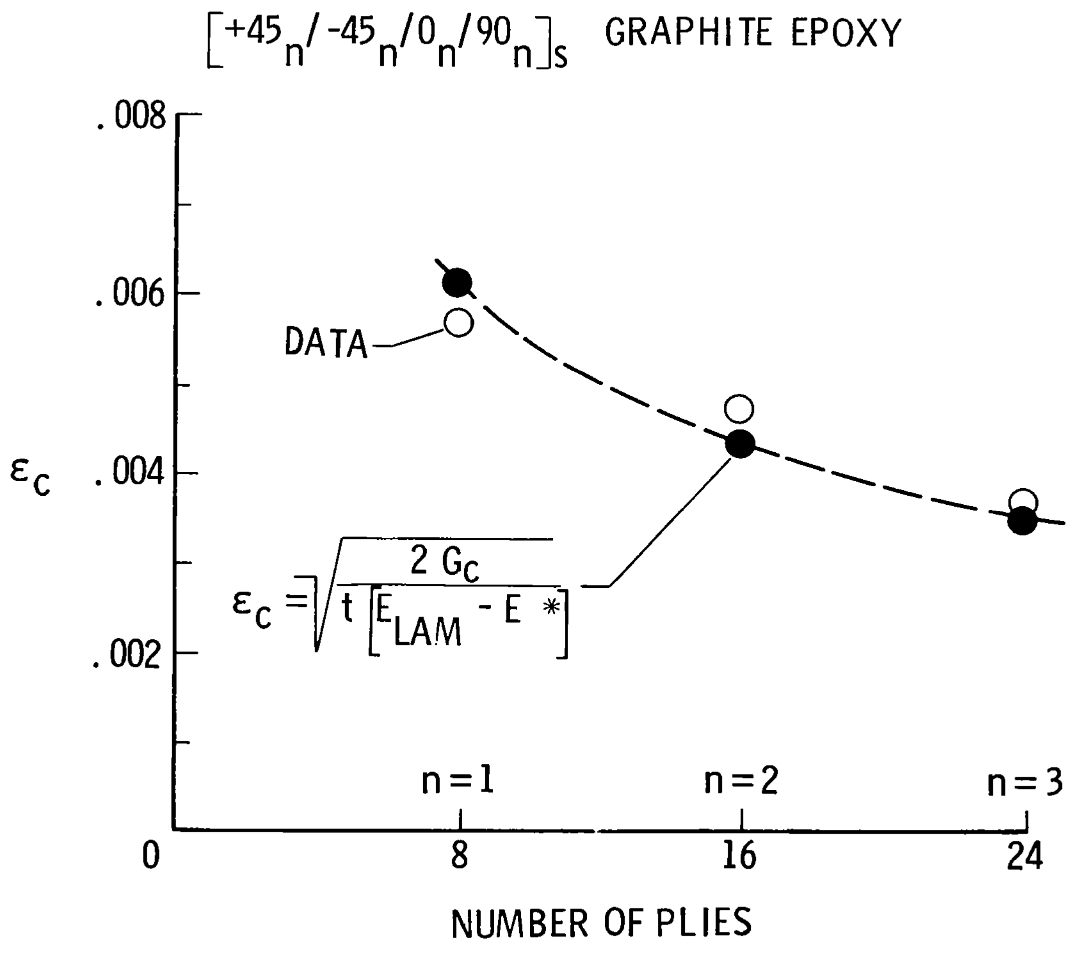

Figure 12

EDGE DELAMINATION TENSION TEST MEASURES

INTERLAMINAR FRACTURE TOUGHNESS

A simple test has been developed for measuring the interlaminar fracture toughness of composites made with toughened matrix resins (ref. 10). The test involves measuring the stiffness, E_{LAM}, and nominal strain at onset of delamination, ε_c, during a tension test of an 11-ply $[\pm 30/\pm 30/90/\overline{90}]_s$ laminate (fig. 13). These quantities, along with the measured thickness t, are substituted into a closed-form equation for the strain energy release rate, G, for edge delamination growth in an unnotched laminate (ref. 9). The E* term in the equation is the stiffness of the $[\pm 30/\pm 30/90/\overline{90}]_s$ laminate if the 30/90 interfaces were completely delaminated. It can be calculated from the simple rule of mixtures equation shown in figure 13 by substituting the laminate stiffness measured during tension tests of $[\pm 30]_s$ and $[90]_n$ laminates. The critical value of G_c at delamination onset is a measure of the interlaminar fracture toughness of the composite. This edge delamination test is being used by Boeing, Douglas, and Lockheed under the NASA ACEE (Aircraft Energy Efficiency) Key Technologies contracts to screen toughened resin composites for improved delamination resistance (ref. 11).

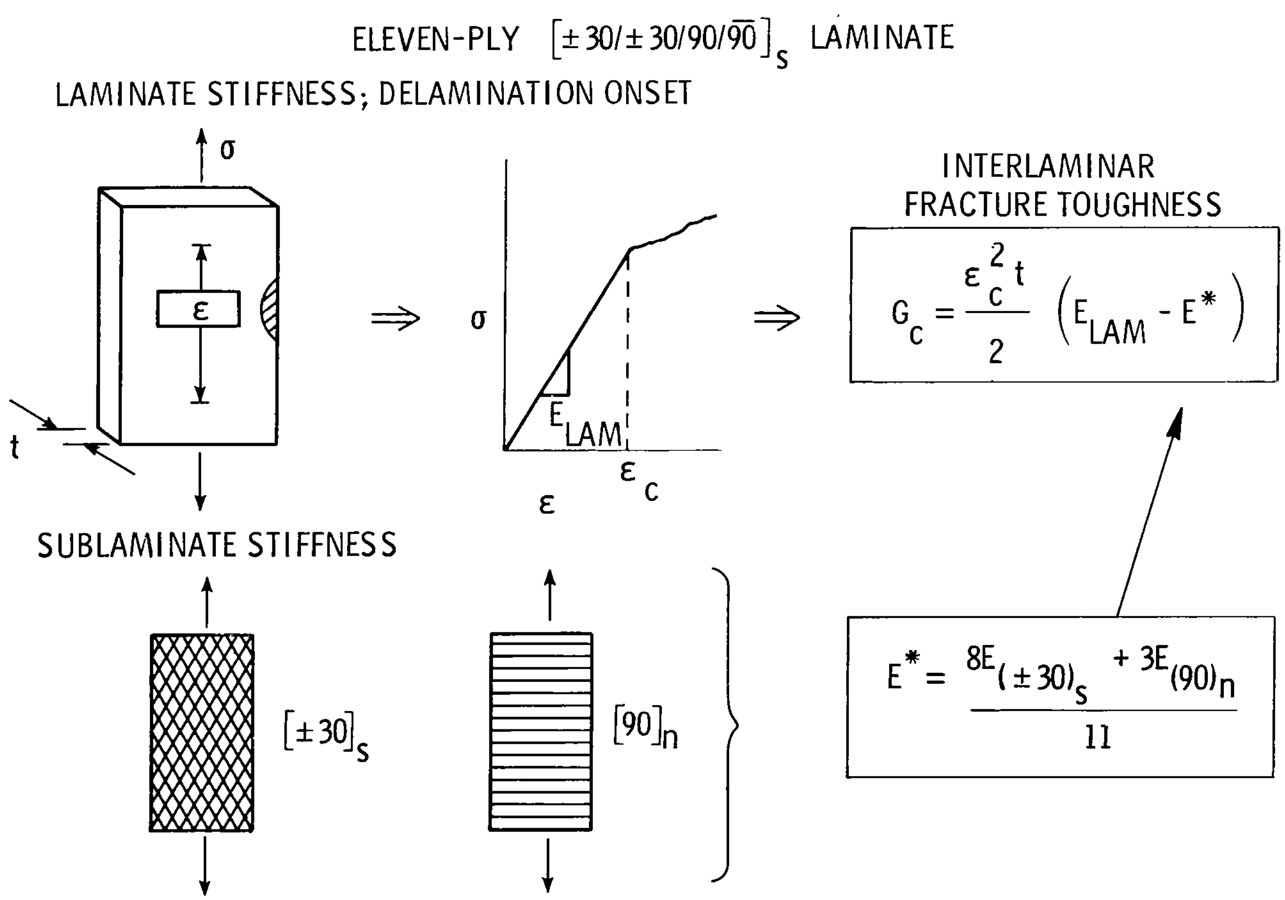

Figure 13

MIXED-MODE STRAIN ENERGY RELEASE RATES DETERMINED

A quasi-three-dimensional finite-element analysis (ref. 12) was performed to determine the relative crack opening (mode I) and shear (mode II) contributions of the $[\pm 30/\pm 30/90/\overline{90}]_s$ edge delamination specimen (ref. 10). Delaminations were modeled in the 30/90 interfaces where they were observed to occur in experiments. Figure 14 indicates that the total G represented by G_I plus G_{II} reaches a value prescribed by the closed-form equation derived from laminated-plate theory and the rule of mixtures. Furthermore, like the total G, the G_I and G_{II} components are also independent of delamination size. In addition, the percentage, G_I/G_{II}, is fixed for a particular layup and does not change significantly for different resin composites as long as the laminates have the same kinds of fibers.

FINITE ELEMENT ANALYSIS OF MIXED MODE PERCENTAGES

$[\pm 30/\pm 30/90/\overline{90}]_s$ LAMINATE

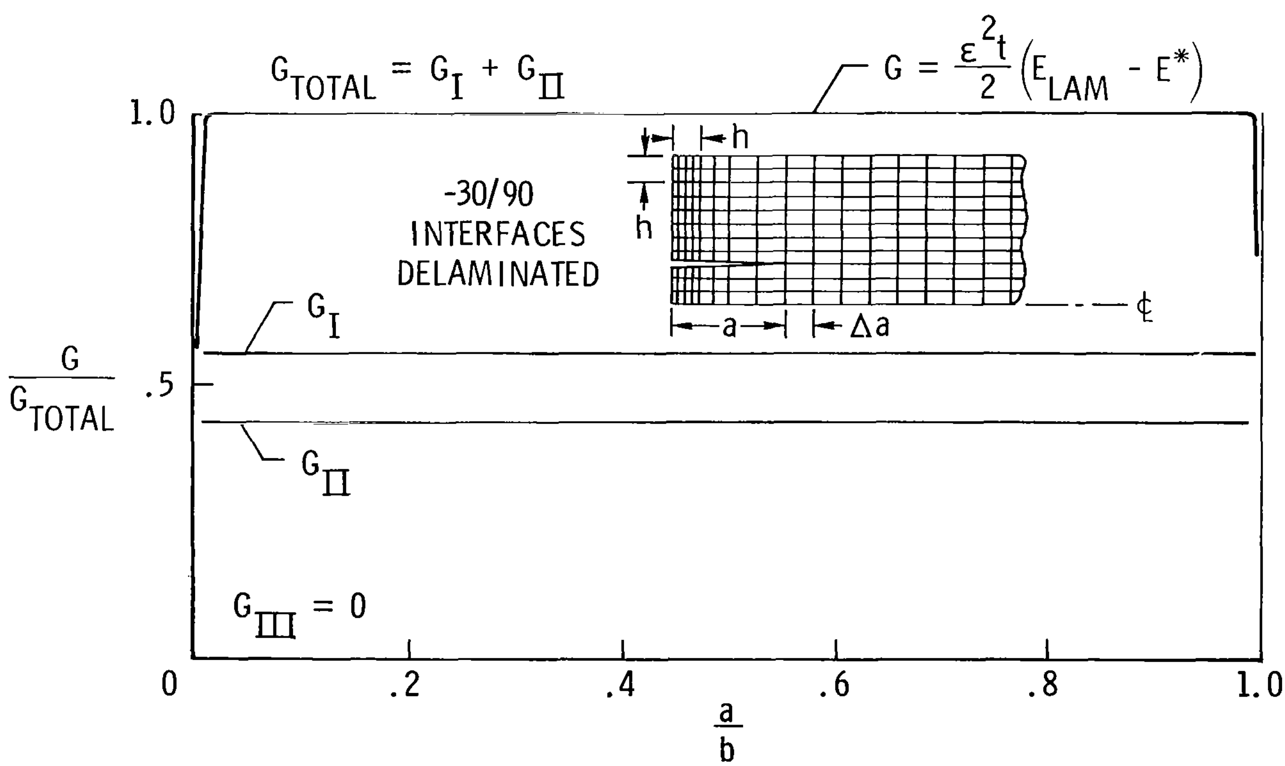

Figure 14

INTERLAMINAR FRACTURE TOUGHNESS OF GRAPHITE COMPOSITES MEASURED

Two test methods are being developed to measure the interlaminar fracture toughness of graphite-reinforced composites (ref. 10). The first is a pure crack opening (mode I) double-cantilever-beam test. The second is the NASA-developed crack opening and shear, mixed-mode (modes I and II), edge delamination tension test (refs. 10 and 11). Figure 15 shows results of these measurements for a relatively brittle 350°F-cure epoxy (5208), a tougher 250°F-cure epoxy (H-205), and a still tougher rubber-toughened 250°F-cure epoxy (F-185). Results indicate that for the brittle epoxy, even in the mixed-mode test, only the crack opening fracture mode contributes to delamination. However, for the tougher 250°F-cure epoxy and its rubber-toughened version, both the crack opening and shear fracture modes contribute to delamination. Hence, although both tests indicate relative improvements among materials, one test alone is not sufficient to quantify interlaminar fracture toughness.

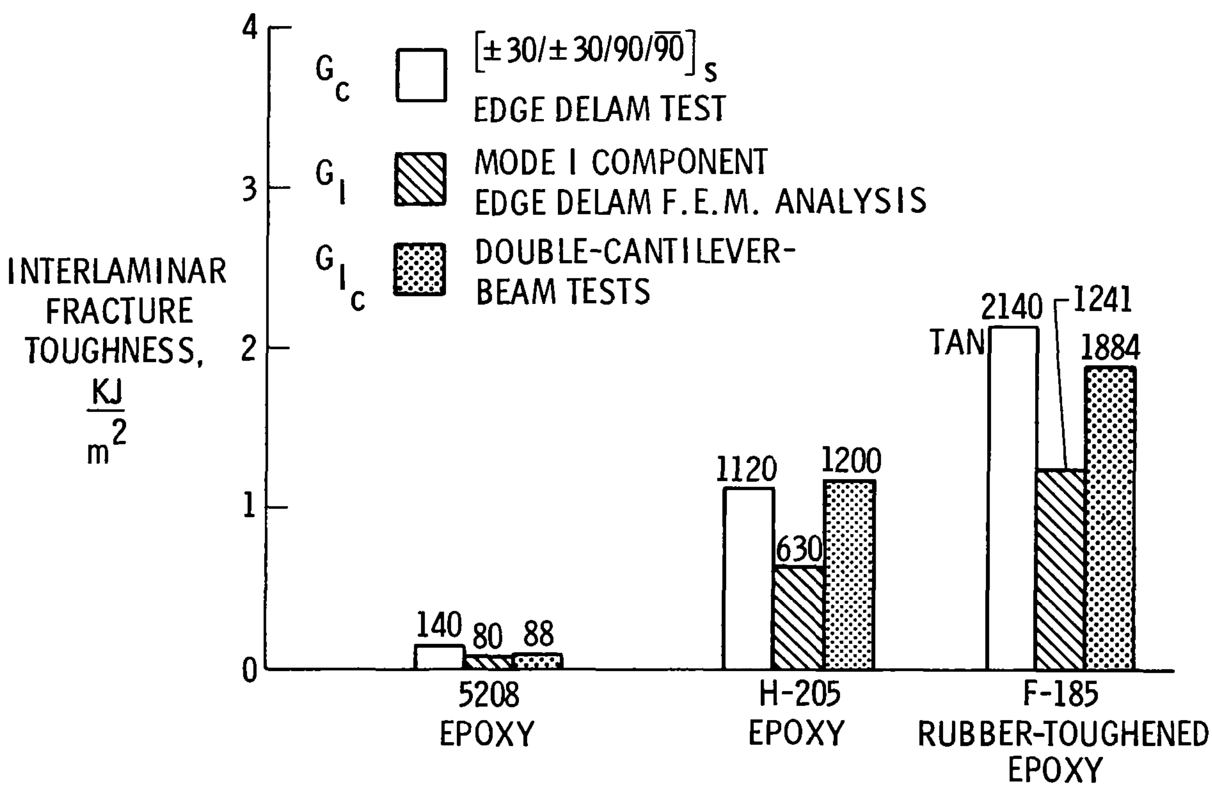

Figure 15

INVESTIGATION OF INSTABILITY-RELATED DELAMINATION GROWTH

Under compression load fatigue, delaminations in composites sometimes induce localized buckling, causing high interlaminar stresses at the ends of the delamination. Rapid delamination growth and loss of structural stability often ensue. Because delamination growth can lead to structural instability, the growth process must be understood. To improve our understanding, through-width delaminations (fig. 16) were studied experimentally and analytically (ref. 13). The figure shows a comparison of measured growth rates and calculated strain energy release rates, which are a measure of the intensity of stresses at the crack tip. In the figure, G_I and G_{II} are the energy release rates related to peel and shear stresses, respectively. Note that both G_I and the growth rate first increase then decrease rapidly with crack extension; G_{II} increases monotonically and does not reflect the change in growth rate. Apparently, the rate of delamination growth is governed by the intensity of the peel stress field. Hence, prediction of crack growth depends on an accurate assessment of the peel stress field around the crack tip. Further work will concentrate on quantifying the relationship between calculated peel stress or related parameters (e.g., G_I) and delamination growth rates.

COMPARISON OF STRAIN-ENERGY-RELEASE RATES AND DELAMINATION GROWTH RATES

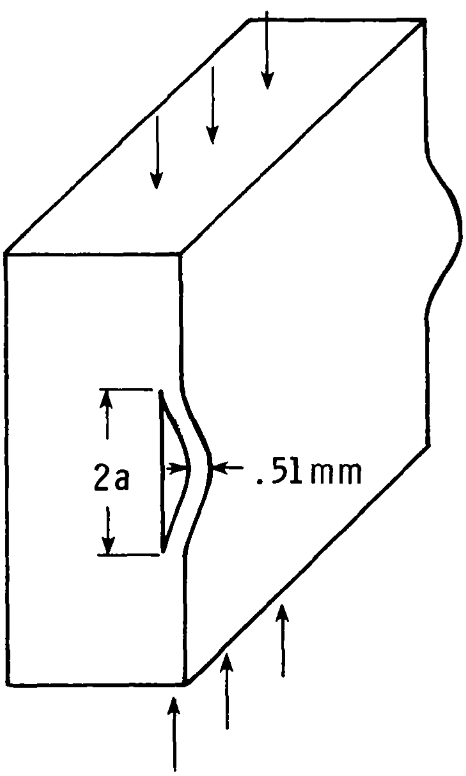

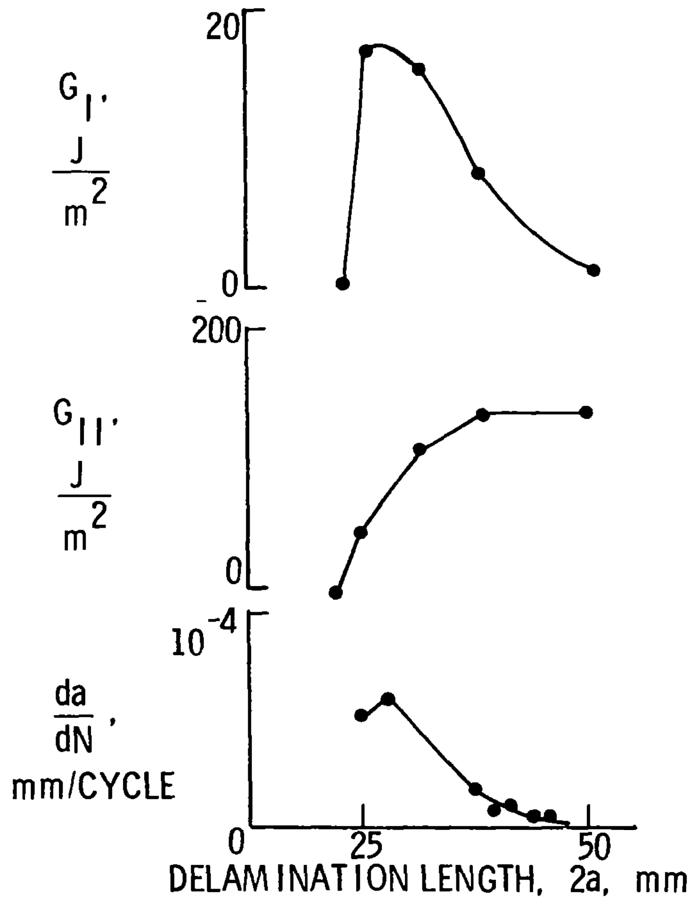

Figure 16

LOCAL DELAMINATION CAUSES TENSILE FATIGUE FAILURES

A study of damage development during tension-tension fatigue loading of unnotched $[\pm 45/0/90]_s$ laminates has demonstrated that local delamination is responsible for fatigue failures at cyclic load levels below the static tensile strength (ref. 14). The circular symbols in figure 17 show the maximum cyclic load, P_{max}, plotted as a function of the number of load-controlled fatigue cycles, N, needed (1) to create delaminations along the edge in 0/90 interfaces (open symbols) and (2) to cause fatigue failures (solid symbols). The arrows extending to the right of data points at or near 10^6 cycles indicate runouts, i.e., no fatigue failures. The square symbols in figure 17 indicate the mean value of (1) load at onset of 0/90 interface delamination along the edge (open symbol) and (2) load at failure (closed symbol) in quasi-static tension tests. During these quasi-static tests, edge delaminations grew almost entirely through the specimen width before failure. Hence, the initial static tensile strength reflects the presence of large 0/90 interface edge delaminations. Yet the endurance limit for fatigue failure was 70 percent of this static tensile strength. Fatigue tests run at cyclic load levels below this limit, but above 40 percent of the tensile strength, contained extensive edge delaminations just like those observed in quasi-static tests. However, specimens in these tests did not fail in fatigue. But tests run at or above the 70-percent endurance limit also developed local delaminations in +45/-45 interfaces. These local delaminations, which originated from matrix cracks in the surface +45° plies, reduced the local cross section and changed the local stiffness. These changes in local stiffness and cross section increased the local strain in the 0° plies, resulting in fiber fracture and laminate failure. Future work will concentrate on predicting fatigue endurance limits using fracture mechanics models of local delamination.

TENSILE FATIGUE BEHAVIOR OF UNNOTCHED $[\pm 45/0/90]_s$ GRAPHITE EPOXY LAMINATES

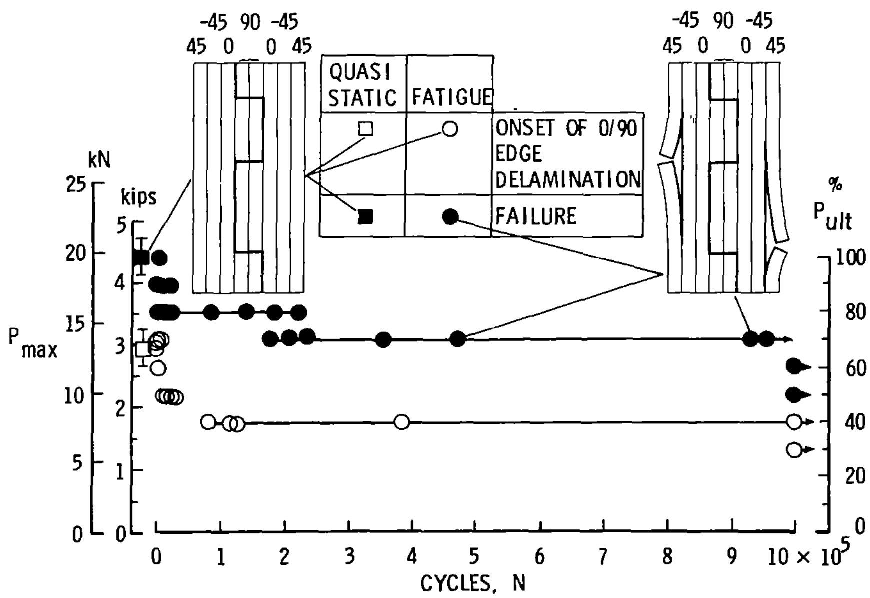

Figure 17

TEST METHODS FOR COMPRESSION FATIGUE OF COMPOSITES

Test methods developed for the fatigue evaluation of airframe metals, primarily aluminum alloys, may not be appropriate for composites. The results of two investigations (ref. 15) aimed at development of test methods for composites loaded primarily in cyclic compression are shown in figure 18. The left side of the figure shows the results of simple cyclic load tests that were conducted to select a method for preventing column buckling in fatigue tests of thin coupons containing an open hole. The test results show that the best configuration is one that does not limit the localized buckling that develops near the hole due to fatigue-induced delaminations. Limiting the localized buckling causes the test to yield an unrealistically long life estimate. The right side of the figure shows the results of simulated flight loading tests that were conducted to determine what parts of the flight load spectrum could be deleted from the simulation to shorten test time without affecting the test result. The results show that deletion of 90 percent of the low loads did not change the test life very much, but that deletion of just a few of the rare, high loads led to very long test lives. Therefore, to be on the safe side in tests on composite structure, the high loads must not be deleted from the test spectrum as would normally be done in tests on aluminum structure.

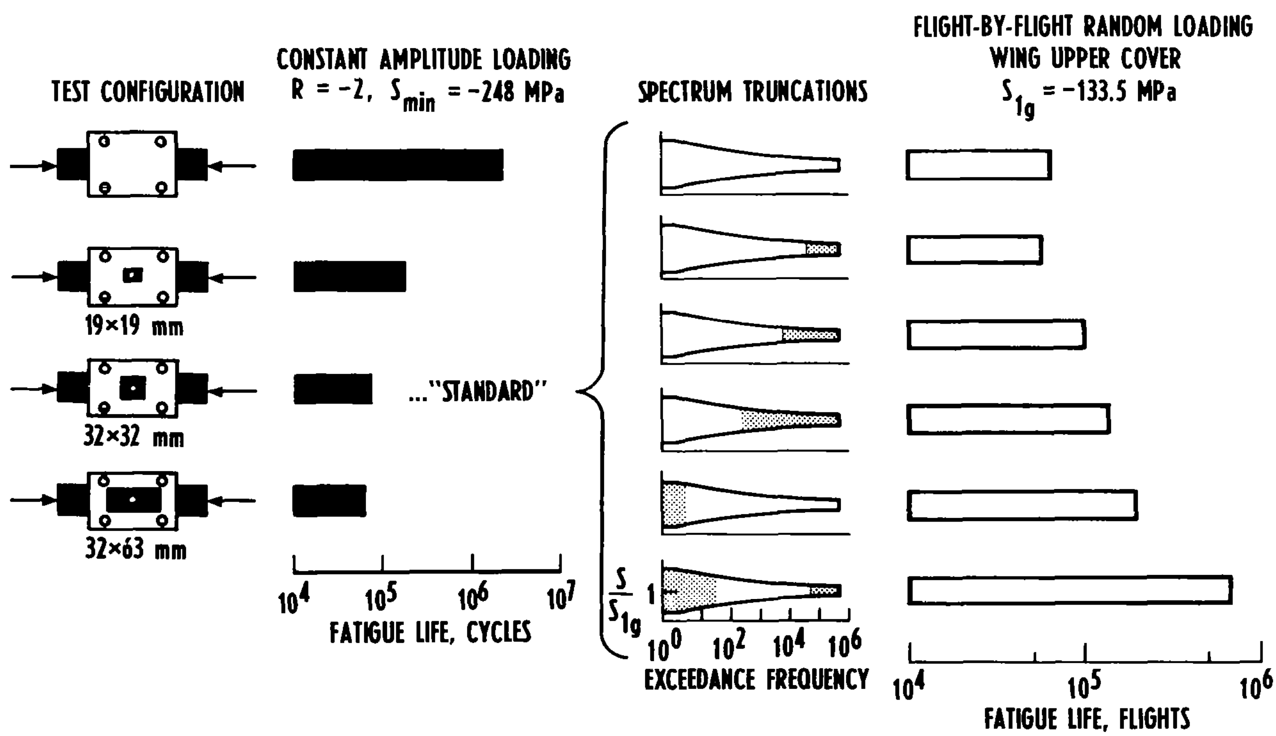

Figure 18

FATIGUE DAMAGE IN BORON/ALUMINUM LAMINATES

Because an aluminum matrix has a modulus 20 times higher than a polymer matrix, matrix cracking in aluminum matrix composites strongly influences laminate stiffness. After long periods of fatigue loading, matrix cracks form in boron/aluminum composites and stiffness may drop significantly (ref. 16). A simple analysis has been developed to predict these laminate stiffness reductions due to fatigue (ref. 17). The analysis is based upon the elastic modulus of the fiber and matrix, fiber volume fraction, fiber orientation, and cyclic-hardened yield stress of the matrix material. It readily predicts the laminate secant modulus of the composite at the stabilized damage state (after approximately 500,000 cycles) for a given cyclic stress range or cyclic strain range. Figure 19 illustrates the agreement between prediction and experiment. The material is $[0_2/\pm 45]_s$ boron/aluminum, with a fiber volume fraction of 0.45. The solid line represents the predicted laminate stiffness loss. Since the relation between cyclic stress range and cyclic strain range does not depend upon stress ratio, either can be used to predict secant modulus degradation. The secant modulus is shown to decrease with increasing stress or strain range. This particular laminate's secant modulus dropped over 40 percent without impending failure. The data were generated under either strain-controlled or load-controlled conditions.

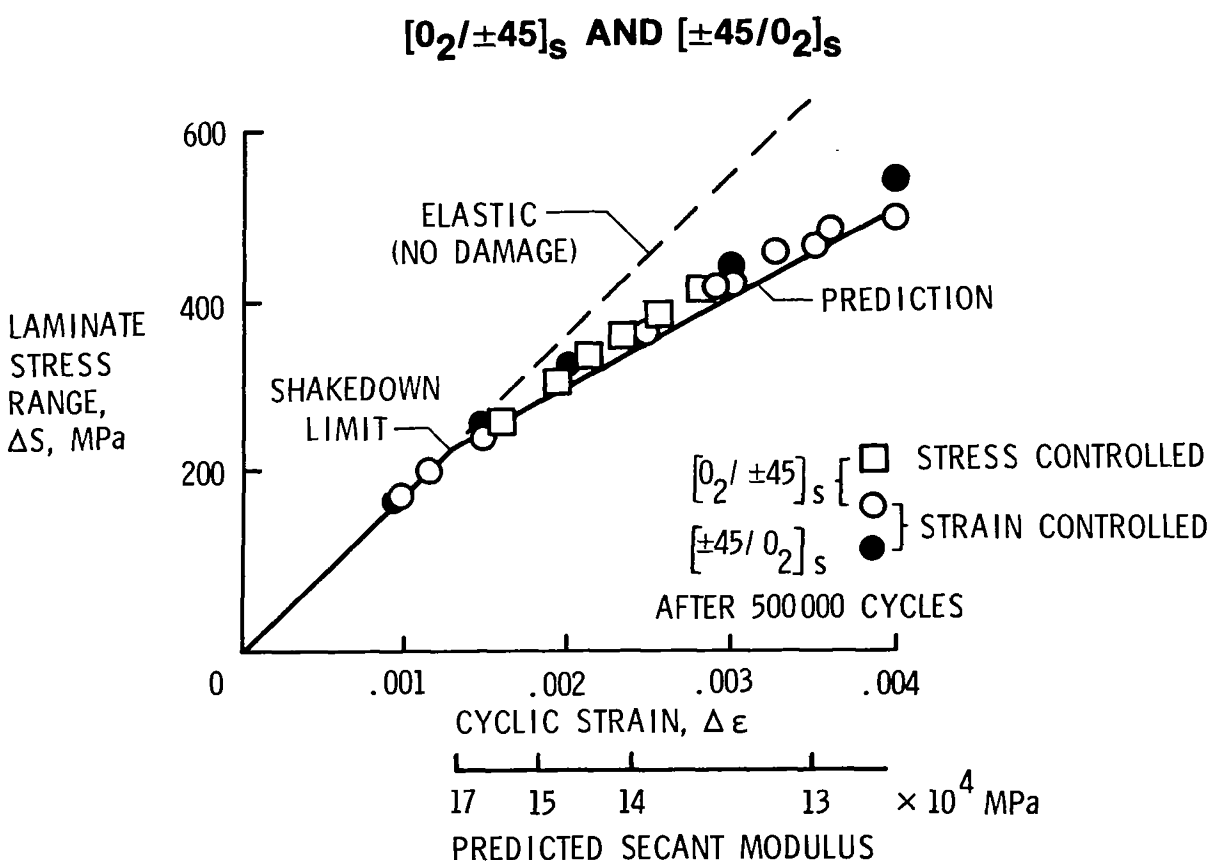

Figure 19

DEBONDING OF ADHESIVELY BONDED COMPOSITES UNDER FATIGUE LOADING

An experimental and analytical investigation based on fracture mechanics methodology was undertaken to study fatigue failure (such as the gradual growth of debonded area when loads are repeated) of adhesively bonded composite joints. A cracked lap-shear specimen was used to test the adhesives. This specimen simulates a realistic adhesive joint where a combination of shear and peel stresses are present. Different configurations of cracked lap-shear specimens are being investigated. The different configurations have different percentages of the strain energy release rate, G, associated with debond opening tension, G_I, and debond shearing, G_{II} (ref. 18). Specimens were made from T300/5208 graphite/epoxy and Kevlar/epoxy (ref. 19). The EC-3445 and FM-300 adhesives tested were cured at 121°C and 177°C, respectively. Specimens are being studied for the combination of both composites and adhesives. For example, figure 20 shows the correlation between the experimentally measured debond growth rate, da/dN, and the value of strain energy release rate, G_I, for the two adhesive systems measured using graphite/epoxy specimens. The FM-300 has a slower growth rate than EC-3445 for an equivalent G_I. The purpose of the program is to develop a model to relate strain energy release rate to debond behavior for any structural geometry. This would then in turn be used to design safe, efficient, bonded composite structures.

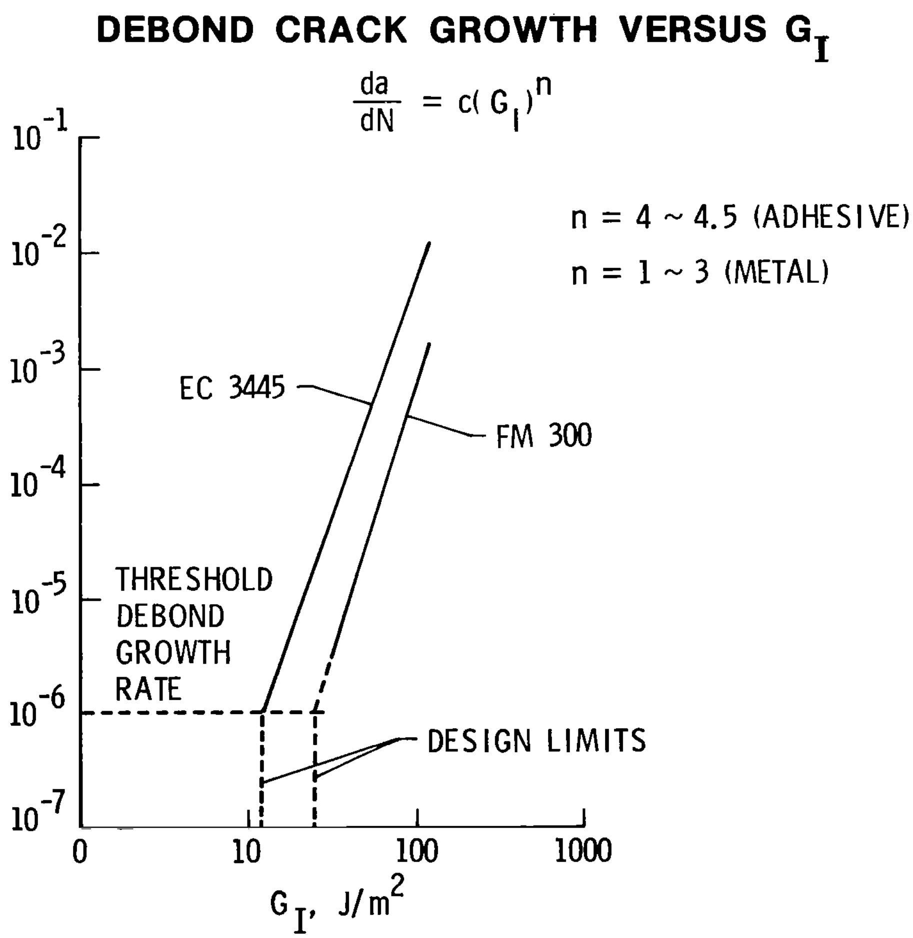

Figure 20

FUTURE WORK

As a result of these recent activities, work is planned in the following areas.

- o Develop analyses for buffer strips with a wide range of parameters.
- o Analyze damage mechanisms for bearing loaded holes.
- o Extend finite-element analysis of bolt clampup to account for transient environments.
- o Extend 3-D finite-element analyses of interlaminar stresses to account for thermal and hygroscopic effects.
- o Determine static and fatigue delamination failure criteria for a variety of mixed-mode loadings.
- o Predict delamination growth due to local instabilities.
- o Predict fatigue endurance limits for arbitrary composite laminates.
- o Predict fatigue endurance limits for adhesively bonded joints.
- o Evaluate second-generation composites for improved delamination and impact resistance.

REFERENCES

1. Poe, C. C., Jr.; and Sova, J. A.: Fracture Toughness of Boron/Aluminum Laminates With Various Proportions of 0° and ±45° Plies. NASA TP-1707, 1980.

2. Poe, C. C., Jr.: A Single Fracture Toughness Parameter for Fibrous Composite Laminates. NASA TM-81911, 1981.

3. Poe, C. C., Jr.; and Kennedy, J. M.: An Assessment of Buffer Strips for Improving Damage Tolerance of Composite Laminates. Journal of Composite Materials Supplement, vol. 14, no. 1, 1980, pp. 57-70.

4. Crews, J. H., Jr.: Bolt-Bearing Fatigue of a Graphite/Epoxy Laminate. Joining of Composite Materials, K. T. Kedward, ed., ASTM STP 749, American Society for Testing and Materials, 1981, pp. 131-144.

5. Shivakumar, K. N.; and Crews, J. H., Jr.: Bolt Clampup Relaxation in a Graphite/Epoxy Laminate. NASA TM-83268, 1982. (Also to appear in Long-Term Behavior of Composites, T. K. O'Brien, ed., American Society for Testing and Materials Special Technical Publication.)

6. Shivakumar, K. N.; and Crews, J. H., Jr.: An Equation for Bolt Clampup Relaxation in Transient Environments. NASA TM-84480, 1982. (Also accepted for publication in Composites Technology Review.)

7. Raju, I. S.; and Crews, J. H., Jr.: Three-Dimensional Analysis of $[0/90]_s$ and $[90/0]_s$ Laminates with a Central Circular Hole. NASA TM-83300, 1982. (Also accepted for publication in Composites Technology Review.)

8. Bostaph, G. M.; and Elber, W.: Static Indentation Tests on Composite Plates for Impact Susceptibility Evaluation. Paper presented at the U.S. Army Symposium on Solid Mechanics: Critical Mechanics Problems in Systems Design (Cape Cod, MA), Sept. 21-23, 1982.

9. O'Brien, T. K.: Characterization of Delamination Onset and Growth in a Composite Laminate. Damage in Composite Materials, K. L. Reifsnider, ed., ASTM STP 775, American Society for Testing and Materials, 1982, pp. 140-167. (Also NASA TM-81940, 1981.)

10. O'Brien, T. K.; Johnston, N. J.; Morris, D. H.; and Simonds, R. A.: A Simple Test for the Interlaminar Fracture Toughness of Composites. SAMPE Journal, vol. 18, no. 4, 1982, pp. 8-15.

11. Standard Tests for Toughened Resin Composites. NASA RP-1092, 1982.

12. Raju, I. S.; and Crews, J. H., Jr.: Interlaminar Stress Singularities at a Straight Free Edge in Composite Laminates. Journal of Computers and Structures, vol. 14, no. 1-2, 1981, pp. 21-28.

13. Whitcomb, J. D.: Finite Element Analysis of Instability-Related Delamination Growth. Journal of Composite Materials, vol. 15, 1981, pp. 403-426.

14. O'Brien, T. Kevin: Tension Fatigue Behavior of Quasi-Isotropic, Graphite/Epoxy Laminates. Fatigue and Creep of Composite Materials, H. Lilholt and R. Talreja, eds., Risø National Laboratory, Roskilde, Denmark, 1982, pp. 259-264.

15. Phillips, E. P.: Effects of Truncation of a Predominantly Compression Load Spectrum on the Life of a Notched Graphite/Epoxy Laminate. Fatigue of Fibrous Composite Materials, ASTM STP 723, American Society for Testing and Materials, 1981, pp. 197-212. (Also NASA TM-80114, 1979.)

16. Johnson, W. S.: Mechanisms of Fatigue Damage in Boron/Aluminum Composites. Damage in Composite Materials, K. L. Reifsnider, ed., ASTM STP 775, American Society for Testing and Materials, 1982, pp. 83-102. (Also NASA TM-81926, 1980.)

17. Johnson, W. S.: Modeling Stiffness Loss in Boron/Aluminum Below the Fatigue Limit. NASA TM-83294, 1982. (Also to appear in Long-Term Behavior of Composites, T. K. O'Brien, ed., American Society for Testing and Materials Special Technical Publication.)

18. Dattaguru, B.; Everett, R. A., Jr.; Whitcomb, J. D.; and Johnson, W. S.: Geometrically Nonlinear Analysis of Adhesively Bonded Joints. Paper presented at 23rd AIAA/ASME/ASCE/AHS Structures, Structural Dynamics, and Materials Conference (New Orleans, LA), May 10-12, 1982. (Also accepted for publication in Journal of Engineering Materials and Technology.)

19. Mall, S.; Johnson, W. S.; and Everett, R. A., Jr.: Cyclic Debonding of Bonded Composites. Paper presented at International Symposium on Adhesive Joints: Their Formation, Characteristics, and Testing (Kansas City, MO), September 13-16, 1982.